Analytical Studies on the Impact of Using Repeated-Rib Roughness in LMR Decay Heat Removal Systems

by

N. T. Obot*, J. H. Tessier and D. R. Pedersen
Reactor Analysis and Safety Division
ARGONNE NATIONAL LABORATORY
Argonne, Illinois 60439

ABSTRACT

A numerical study was carried out to determine the effects of roughness on the thermal performance of Liquid Metal Reactor (LMR) decay heat removal systems for a range of possible design configurations and operating conditions. The ranges covered for relative rib height (e/D_h), relative pitch (p/e) and flow attack angle were 0.026-0.103, 5-20 and 0-90 degrees, successively. The heat flux was varied between 1.1 and 21.5 kW/m^2 (0.1 and 2.0 kW/ft^2). Calculations were made for three cases: smooth duct with no ribs, ribs on both the guard vessel and collector wall, and ribs on the collector wall only. The results indicate that significant benefits, amounting to nearly two-fold reductions in guard vessel and collector wall temperatures, can be realized by placing repeated ribs on both the guard vessel and the collector wall. The magnitudes of the reduction in the reactor vessel temperature are considerably smaller. In general, the level of improvement, be it with respect to temperature or heat flux, is only mildly affected by changes in rib height or pitch but exhibits greater sensitivity to the assumed value for the system form loss. When the ribs are placed only on the collector wall, the heat removal capability is substantially reduced.

*On sabbatical leave from Clarkson University, Potsdam, New York.

1. INTRODUCTION

The use of natural-circulation flow of air to effect shutdown heat removal from the reactor vessel is one of the main features of the advanced liquid metal reactor (LMR) cooling concepts. With this cooling scheme, which is inherently reliable and entirely passive in that it requires no operator action, it is possible to maintain component temperatures at acceptable limits. Also, heat transfer rates on the air-side can be improved markedly by using fins or repeated ribs on the outside of the guard vessel and the collector wall or on either of these two walls. The work described in this report was motivated by the need to solve problems relevant to effective design of shutdown heat removal systems (SHRS) for liquid metal reactors. Its objective was to determine the impact of use of repeated ribs on shutdown heat removal capability. The systems under consideration are the Reactor Vessel Auxiliary Air Cooling Systems of General Electric's PRISM reactor and Rockwell International's SAFR reactor. In these systems the decay energy is removed by a naturally convecting air stream from the guard "containment" vessel. Typical peak values of heat flux for the PRISM and SAFR reactors are of the order of 10-12 kW/m^2.

Consistent with the design of the Argonne Natural Convection Shutdown Heat Removal Test Facility (NSTF), which simulates the annular flow passage between the guard vessel and the collector wall (Fig. 1) using a rectangular duct of aspect ratio 4.33; analytical studies have been carried out using existing correlations for friction and heat transfer obtained on ducts having two rough walls (Han et al., 1978; 1979). A very thorough analysis has been made for the option with repeated ribs on both the collector wall and the guard vessel. The geometric parameters considered included the rib height (e), pitch (p), flow attack angle (α, angular orientation with respect to the flow), and the gap size between the guard vessel and the collector wall.

The option of placing the ribs only on the collector wall was also examined. This aspect of the analysis was not as exhaustive as one would wish, due to lack of predictive equations for friction and heat transfer for rectangular channels having one rough wall. Also, for the purposes of comparison, revised calculations for the smooth duct option were made by allowing for the dependence of friction factor and heat transfer coefficient on the duct aspect ratio (Jones, 1976; Obot, 1987).

ANALYSIS AND CALCULATION PROCEDURES

This section gives a discussion of the assumptions made and of the correlations as well as the procedural steps used in the analysis.

In addition to the specific modifications and assumptions to be discussed subsequently, the common feature of all calculations was the lumped parameter model. Specifically, the thermal driving head and the system pressure losses were given by Equations (1) and (2):

$$\Delta P_h = \rho_o g \left[(1 - \bar{\rho}/\rho_o) L_h + (1 - \rho_s/\rho_o) L_s \right] \tag{1}$$

$$\Delta P_L = \frac{G^2}{2\rho_o} \left\{ (\rho_i/\rho_o) K_L + (2 f_h L_h/D_h)(T_a/T_o + 1) \right.$$

$$\left. + (4 \rho_o f_s L_s/\rho_s D_{hs}) (A_{fh}/A_{fs})^2 + (T_a/T_o - 1) \right\} \tag{2}$$

where

$$K_L = K_{L,i} (A_{fh}/A_{fi})^2 \tag{3}$$

In Eq. (3), the subscript i refers to local geometric conditions in the system and $K_{L,i}$ is a constant with an appropriate value for the geometric change. The overall form loss coefficient, K_L, is the sum of entrance and exit losses outside of the heated zone and it is expressed in terms of the inlet velocity head. The first and second terms on the RHS of Eq. (1) correspond to the driving heads in the heated and stack zone, respectively. Beginning from left to right, the four terms on the RHS of Eq. (2) represent the contributions due to form loss, friction in the heated and stack zones, and acceleration pressure loss. The standard assumption was that the thermal driving head is exactly balanced by the sum of the system pressure losses, i.e., $\Delta P_h = \Delta P_L$. Hence, the flowrate, average air density and exit temperature were determined iteratively from assumed initial guesses for flowrate, wall and exit temperatures.

To obtain steady state temperatures, the following heat transfer relations were used:

$$Q_w = h_{GV} (T_{GV} - T_o) + h_{CW} (T_{CW} - T_o) \tag{4}$$

where

$$h_{CW} (T_{CW} - T_o) = \frac{\sigma (\bar{T}_{GV} - \bar{T}_{CW})}{\frac{1}{\varepsilon_{GV}} + \frac{1}{\varepsilon_{CW}} - 1} \tag{5}$$

The average reactor vessel temperature, $\bar{T}_{RV}$, was related to Q_w by

$$\bar{T}_{RV} = [\bar{T}_{GV} + \frac{Q_w}{\sigma} (\frac{1}{\varepsilon_{RV}} + \frac{1}{\varepsilon_{GV}} - 1)]^{1/4} \tag{6}$$

while the temperature of air at the exit of the heated zone was calculated from:

$$T_a = T_o + Q_w L_h / G C_p H \tag{7}$$

Surface emissivities were held fixed at 0.7 for all cases and h_{GV} was set equal to h_{CW}, except when dealing with the case for which the ribs were located only on the collector wall.

For the smooth duct option, friction factor (f_s) and Nusselt number for the rectangular channel were computed from equations (8) and (9).

$$\bar{f}_s = (1.58 \ln \bar{R}e - 3.82)^{-2.0} \tag{8}$$

$$\bar{N}u_s = (\bar{f} \cdot \bar{R}e \cdot Pr/2)[1.07 + 12.7 (\bar{f}_s/2)^{1/2}(Pr^{2/3} - 1)]^{-1.0} \tag{9}$$

where

$$\bar{R}e = \phi^*(W/H)Re \tag{10}$$

Re = Reynolds number based on D_h

$$\phi^*(W/H) = \frac{2}{3} + \frac{11}{24}\frac{H}{W}\left(2 - \frac{H}{W}\right) \tag{11}$$

From equations (8)-(11) it is clear that corrections have been applied to the familiar circular tube relations to account for the dependence of friction factor (Jones, 1976) and heat transfer coefficient (Obot, 1987) on aspect ratio.

With repeated-rib roughness, friction factor and Nusselt number were calculated from the following correlations given by Han et al. (1978).

$$B^+ = 4.9\,[(\phi/90^o)^{0.35}\,(10/p)^n\,(\alpha/45^o)^{0.57}]^{-1.0}\ ;\ \text{for } e^+ \geq 35 \tag{12}$$

$$Nu_r = f_r \cdot Re \cdot Pr\,[(H^+ - B^+)(2f_r)^{1/2} + 2]^{-1.0} \tag{13}$$

where

$$n = \begin{cases} -0.13, & 5 \leq p/e < 10 \\ 0.53\,(\alpha/90°)^{0.71}, & 10 \leq p/e \leq 20 \end{cases}$$

$$B^+ = (2/f_r)^{1/2} + 2.5\,\ln(2e/D_h) + 3.75 \tag{14}$$

$$e^+ = (e/D_h)Re\,(f_r/2)^{1/2} \tag{15}$$

or
$$H^+ = 8(e^+/35)^{0.28}/(\alpha/45°)^y \tag{16}$$

$$y = \begin{cases} 0.5, & \alpha < 45° \\ -0.45 & \alpha \geq 45° \end{cases}$$

Equations (12)-(16) correspond to those reported by Han et al. in their original paper. In this regard it may be noted that Han et al. (1979) re-analyzed their data by replacing the constant (3.75) on the RHS of Eq. (14) by 4.23, as the latter is usually considered to be more appropriate for rectangular geometry. Although the constants and exponents in the revised correlations are slightly different from those associated with the above

equations, the calculated friction factors or heat transfer coefficients are quite insensitive to this modest change in the numerical value for the constant. In fact, the original, Equations (12)-(16), and the revised (not quoted here) correlations give results that differ by no more than one percent. For example, with $p/e = 10$, $\alpha = 45°$ and $e^+ = 50$, the calculated friction factors for the original and revised correlations are 0.0311, 0.0309 for $e/D_h = 0.0302$; 0.0456 and 0.0453 for $e/D_h = 0.056$; 0.0762 and 0.0756 for $e/D_h = 0.102$. Likewise, for the same conditions, the calculated Stanton numbers were essentially the same, being within 0.0001 for all three e/D_h values. Based on a very thorough comparative evaluation of the revised and original correlations, we recommend the latter, especially since two different heat transfer equations were provided.

There are several additional comments. First, the full scale simulations were carried out for $e^+ \geq 35$, as this is the applicable range for the present situation. In fact, over a wide range of assumed geometric and flow conditions, the lowest e^+ value was about 200. Also, no correction, similar to that applied to the smooth duct Reynolds number, was made partly because friction factor or heat transfer in the fully rough regime is quite independent of Reynolds number and partly because the general form of the corrections for roughened passages is unknown. And, further, the ribs were assumed to be of square cross-section; hence the profile shape angle, ϕ, in Equation (12) was set to 90 degrees for all cases.

The equations and changes noted in this section were incorporated into the computer program used to study the smooth duct heat removal scheme. A summary of the parametric ranges covered in the analysis is given in Table 1. For p/e, calculations were made for $p/e = 0$ ($\alpha = 0$, $e/D_h = 0$, smooth duct option) and $p/e \geq 5$, in increments of 2.5. Concerning the flow attack angle

(α), numerical results were obtained for $20° \leq \alpha \leq 50°$, in increments of 5 degrees, and for 60, 75 and 90 degrees.

RESULTS AND DISCUSSION

It should be noted as a matter of particular importance to the present considerations that, due to the requirement that $\Delta P_h = \Delta P_L$, changes in heated zone friction or system form loss coefficient (sum of entrance and exit losses outside of the heated zone in terms of inlet velocity head) have direct effects on the calculated mass flowrate through the system. It is equally important to note that the results, to be presented hereafter, were obtained for the NSTF geometric conditions with channel width (W) and gap size or spacing (H) of 1.32 m and 0.305 m, respectively. With these specifications, the hydraulic diameter ($D_h = 4A_{fh}/P_w$), which is used for scaling of the rib height (e), has a value of 0.5 m. The only exception to this consistent procedure occurred when analyzing the effect of guard vessel to collector wall gap size and the two figures dealing with these results are given in the second section.

Effects of Repeated-Ribs on Mean Flow Parameters

Naturally, since the impact of roughness on heat transfer rates or wall temperatures depends, to a marked extent, on the prevailing flow conditions, the effects of the rib geometric details and form loss coefficient on mean flow parameters were charted in sufficient detail. These results were too numerous and, due to space limitations, only one such plot is given here on Fig. 2. Here, the heated zone pressure loss scaled with the total system pressure loss is plotted against the helix angle and the results are shown for

five values of e/D_h. To render the subsequent presentation and discussion of the temperature and heat flux data intelligible, the most significant observations on the mean flow are summarized below:

1. For a given rib-height (e/D_h), K_L and α, mean velocity or mass flowrate decreases from its largest value obtained with a smooth duct ($p/e = 0$), attains a minimum at $p/e = 10$ which is also the value that affords maximum friction factor, and then rises gradually as p/e is further increased.

   For a fixed thermal driving head, p/e and α, the total system pressure loss increases with increasing form loss coefficient (K_L) or rib height (e/D_h); hence mean velocity or mass flowrate through the system decreases monotonically with K_L or e/D_h.

3. When p/e, K_L and e/D_h are specified, mean velocity decreases consistently with increasing flow attack angle (α) due to the monotonic increase of heated zone friction factor and hence the pressure loss with α.

4. For a smooth duct, form losses account for much of the system pressure losses. In the presence repeated ribs and for $0.05 < e/D_h \leq 0.103$, system pressure losses are dominated by friction in the heated zone for moderate K_L values in the range $1 \leq K_L \leq 5$ while, for $5 < K_L < 10$ and $0.03 \leq e/D_h \leq 0.05$, the contributions due to friction in the heated zone are about the same as those due to form loss. For $K_L \geq 10$ and $e/D_h > 0.3$, system pressure losses are dominated by form losses.

5. Pressure drop in the stack zone and acceleration pressure loss constitute very small fractions of the system pressure losses,

regardless of whether the duct is smooth or has repeated ribs, and the effects of rib geometric configurations or form loss on stack zone friction or acceleration loss manifest themselves through variations in mass flowrate and air density or temperature.

6. When e/D_h and α are specified, frictional pressure coefficient in the heated zone is fixed, independent of the assumed value for K_L or p/e over the ranges $1 \leq K_L \leq 20$ and $5 \leq p/e \leq 20$ even though there are marked effects on mass flowrate. This is due to the fact that friction factor in the fully rough regime is quite independent of flow velocity.

Effects of Repeated-Ribs on Temperatures with Specified Fluxes

In this section the impact of repeated ribs on mean temperatures for the reactor and guard vessel, collector wall and on exit air temperature will be presented graphically. Prior to such a presentation, several comments on the effects of rib geometric parameters and form loss coefficient on heat transfer coefficient are necessary because these have direct bearing on the results to be shown subsequently. First, for any particular K_L, e/D_h or α, a pitch-to-height ratio of 10 afforded maximum values in heat transfer coefficient, with h decreasing very gradually as p/e was increased or decreased beyond this value. Second, for a given e/D_h, p/e, and K_L, a typical h vs. α profile passed through a maximum around α = 45 degrees, as was reported by Han et al. (1978) in their paper. And, further, h increased only moderately with increasing e/D_h, a trend that is consistent with the available literature (Gomelauri, 1964; Webb et al., 1971; Vilemas and Simonis, 1985), but exhibited greater sensitivity to the assumed K_L value. It may also be noted that, for $0.026 \leq e/D_h \leq 0.103$ and depending on the assumed value for K_L, increases in

heat transfer coefficient of 200-400% were calculated with ribs on both the guard vessel and collector wall.

Since α = 45 degrees affords a maximum in heat transfer coefficient and minima in mean wall temperatures, many of the results to be shown subsequently were obtained with this value of flow attack angle. Also, unless stated otherwise, the results are for an assumed guard vessel heat flux of 10.76 kW/m^2 (1.0 kW/ft^2). And, further, it is useful to recall from the discussion at the beginning of the section on results and discussion that, with the exception of Figures 5 and 6 of this section, the remaining results were obtained for the NSTF geometric conditions with channel width (W), gap size (H) and D_h of 1.32 m, 0.305 m, 0.5 m, successively.

Figure 3 is a plot of the average guard vessel temperature against p/e for e/D_h = 0.026, 0.051 and 0.103 (i.e., e = 0.5, 1.0 and 2.0 inch with D_h = 1.625 ft). For clarity, due to the crowding of the curves for all e/D_h, the profiles for e/D_h = 0.039 and 0.077 have been omitted from this figure. Relative to the data for the smooth duct option (p/e = 0), the reductions in mean temperature are quite significant, with very little effect of e/D_h or p/e. Similar mild effects of e/D_h on temperature were established for the reactor vessel, duct wall and exit air.

The four plots of Fig. 4 show the effects of varying the form loss coefficient over the range of values between K_L = 1 and K_L = 20 on mean temperatures for the reactor and guard vessel, collector wall and for the exit air. In examining the gross effects of K_L it must be noted that in going from K_L = 1 to K_L = 20, the air flowrate through the system is reduced by roughly a factor of two. Clearly, the general trend on this figure is one of monotonic increase of all temperatures with K_L; an indication that, in absolute terms, heat flux would decrease as K_L is progressively increased. When the results

for the reactor and guard vessel are viewed in terms of the drop in temperatures over that for the smooth duct option, the magnitudes of the reductions in temperature increase with increasing K_L. For the collector wall, which is located farther from the heat source, the reductions in temperatures are substantially greater, with an average drop of about 400% when K_L is varied between 1 and 20.

Figures 5(a) and 5(b) show the effects of varying the heated zone gap size between the guard vessel and collector wall on mean temperatures. It should be emphasized that, for both figures, the overall form loss coefficient (K_L) was held fixed at 10. For the results on Fig. 5(a), the rib height (e) was held fixed at 25.4 mm (1.0 inch) and with H = 0.152, 0.229, 0.305, 0.381 and 0.457 m (i.e., H = 6, 9, 12, 15 and 18 inches) the corresponding values for e/D_h were: 0.093, 0.065, 0.051, 0.043 and 0.037. With knowledge of D_h for a given W and H, calculations were also carried out with adjustments in e and p to give same p/e (= 10) and e/D_h (= 0.093), and these results are presented on Fig. 5(b). In each figure, beginning from top to bottom, the first three curves for the reactor vessel (RV), guard vessel (GV) and collector wall (CW) are for the smooth duct option, while the last three profiles (in the same order) were obtained with repeated ribs.

Clearly, whether the physical height (e) or e/D_h is held fixed, the outcome of the analysis is the same, that is, in the presence of ribs no significant benefits can be realized by reducing the current gap size of 0.305 m (12 inches) down to 0.152 m (6 inches) or 0.229 m (9 inches). For example, for the same e/D_h, the difference in mean guard vessel temperature between 0.305 m and 0.152 m is about 30°F. This lack of strong influence of gap size reflects the fact that the absolute effect of roughness on heat transfer is greatest near transitional-to-moderate Reynolds numbers, decreases

very slightly with increasing Re and then levels off at very large values of Reynolds number. Vilemas and Simonis (1985) reported that heat transfer rate in the region of partially rough flow conditions depends markedly on e/D_h, while the fully rough regime heat transfer is practically independent of both e/D_h and the configuration of the roughness and is twice that for smooth channels. Although mean velocity decreases with decreasing gap size, the Re or e^+ values for all gap sizes fall within the fully rough regime; hence there are small effects on heat transfer coefficient and on mean temperatures.

To carry the analysis and discussion of the impact of guard vessel to collector wall gap size on mean temperatures a stage further, additional calculations were made but, this time, the variation of K_L with flow area was accounted for using Eq. (3); the reference was the NSTF flow area of 1.32 m^2. Also, using the appropriate equations provided in Bird et al. (1960) for sudden expansion and contraction, allowances were made for form losses due to contraction and/or expansion as the gap size (H) was varied between 0.152 m and 0.457 m (6 and 18 inches). For H = 0.152, 0.229, 0.305, 0.381 and 0.457 (6, 9, 12, 15 and 18 inches), the effective K_L (including contraction and/or expansion effects) values were 3.17, 5.99, 10, 15.69 and 22.61, successively. As with Fig. 5(b), the calculations were carried out for p/e = 10, e/D_h = 0.093, α = 45° and Q_w = 1.0 kW/ft^2 and the results are presented on Fig. 6.

In sharp contrast to the trend on Fig. 5 for a fixed K_L, the smooth duct mean temperatures of Fig. 6 increase markedly with gap size, in line with the trend already documented on Fig. 4 for p/e = 0 and four values of K_L. The profiles on Fig. 5 show that temperature reductions of about 160°F, 200°F and 220°F for the reactor vessel, guard vessel and collector wall may be achieved by halving the current gap size of 12 inches. From Fig. 6 it is especially noticeable that the magnitudes of the drop in temperatures are considerably

larger, with reactor vessel, guard vessel and collector wall reductions of 350°F, 450°F and 520°F when the smooth duct gap size is reduced by a factor of 2. With repeated ribs the general trend with increasing H is about the same as that on Fig. 5, with no significant effects of gap size. Specifically, the differences in mean temperatures between H = 0.152 (6 inches) and 0.305 m (1 ft) are 32°F for the reactor vessel and 80°F for the guard vessel or collector wall.

In summary, the results of an exhaustive analysis of the impact of varying the guard vessel to collector wall gap size on temperatures indicate a significant effect with the smooth duct option, but wall temperatures are less sensitive to variations in gap size with repeated-rib roughness. For example, differences in mean temperatures between the 0.152 m and 0.305 m gap sizes are about 10-80°F for optimum rib pitch and flow attack angle, depending of course on e/D_h and K_L. The practical aspect of this lack of strong effect of gap size on temperatures relates to tolerance in fabrication of the guard vessel to collector wall spacing, inasmuch as small deviations in such specifications should have little impact on the thermal performance.

The compact graphical illustrations on Figs. 7(a) and 7(b) complement one another and show alternative representations of the same data; as mean temperatures versus heat flux and against the Reynolds number. In each figure, results are shown for the smooth duct option and with the ribs; the latter are for e/D_h = 0.051, p/e = 10 and α = 45 deg. For these calculations, heat flux was purposely varied to include values both unusually low and high. The impact of ribs is quite evident and requires no elaboration beyond noting that, even at an excessive wall heat flux corresponding to 21.5 kW/m^2 (2 kW/ft^2), the average temperature for the guard vessel is under 1100°F while that for the reactor vessel is slightly higher.

For the results presented so far, the air temperature at the inlet was held constant at 21.1°C (70°F). Calculations were made to determine the influence of inlet air temperature using a value of 0°C. The guard vessel heat flux was varied between 1.1 and 21.5 kW/m^2. Although all temperatures were lower with 0°C than with 21.1°C, the magnitudes of the reduction in mean wall temperatures were essentially the same, unaffected by this modest change in inlet air temperature.

Finally, additional calculations were made to determine the effect of placing the ribs only on the collector wall with a smooth guard vessel. However, an extensive search of the literature failed to reveal friction or heat transfer correlations for channels having one rough wall, a situation that hampered attempts to analyze the problem more thoroughly. To obtain estimates of the temperatures, three assumptions were made. First, heat transfer coefficient for the smooth guard vessel was taken to be that for a smooth channel and this was obtained using Eq. (9). Second, friction factor with one rough wall was obtained by reducing the value with two rough walls by 50% under identical geometric and flow conditions. Third, heat transfer coefficients for the rough collector wall were calculated from the expressions for two rough walls.

Figure 8 shows a typical variation of mean guard vessel temperature with heat flux. On this figure the notations 1R and 2R refer to the results with ribs on one wall and two walls, respectively. The other conditions for the analysis were: $p/e = 10$, $K_L = 10$, $\alpha = 45$ deg. and $e/D_h = 0.051$. The magnitudes of the reductions in mean temperatures with ribs on the collector wall, though not as large as with ribs on two walls, are quite encouraging in light of the following observation. The predictions are clearly on the conservative side because there are indications that, in the presence of two

rough walls, local heat transfer coefficients for the smooth walls can be 20-50% higher than when all four walls are smooth (Han and Park, 1986). Effects such as these are sufficient to cause further reductions in temperatures beyond those documented here. Appropriate correlations for friction and heat transfer coefficient would be needed before definite conclusions could be made concerning the impact of placing ribs only on the collector wall.

Heat Removal Capability at Constant Reactor Vessel Temperature

It has already been noted that the results in the preceding section were obtained with an assumed guard vessel heat flux of 10.76 kW/m^2, as well as by varying this flux between 1.1 and 21.5 kW/m^2. Of the several drawbacks with this approach, one is that it can result in unusually high temperatures for large form loss coefficients; notably for the smooth duct option which forms the basis for comparison of the effects of repeated ribs. The second is that it does not provide a clear idea of the magnitudes of the heat flux that can be removed with or without the ribs. To shed some light on the latter, additional calculations were made but, this time, the average reactor vessel temperature was specified and the thermal analysis proceeded as before to determine the wall heat flux, the temperatures for the guard vessel, collector wall and the exit air. With this approach the enhancement factor is given simply, without ambiguity, as the ratio $Q_{w,r}/Q_{w,s}$, where $Q_{w,r}$ and $Q_{w,s}$ are the fluxes with and without the ribs. For these trials, the flow attack angle was held fixed at 45 degrees.

Figure 9 shows the effects of form loss coefficient, K_L, on the wall heat flux (Q_w) and mean guard vessel temperature for $\bar{T}_{RV}$ = 1000°F and e/D_h = 0.051 (i.e. e = 25.4 mm). The influence of rib height on Q_w is presented in Fig. 10, while that of varying the reactor vessel temperature is shown differently

on Figs. 11(a) and 11(b), the latter being a plot of $Q_{w,r}/Q_{w,s}$ against p/e. Since there are no large effects of e/D_h on Q_w or temperatures, as might have been expected from the presentation and discussion of Fig. 3, profiles for guard vessel and collector wall mean temperatures are also included in Fig. 10 only for e/D_h = 0.103. Also, to provide quantitative estimates on the heat removal capability, the heat flux ratios for all K_L, three values of e/D_h and p/e = 10 are summarized in tabular form in Table 2.

With respect to the effects of p/e the curves in each of Figs. 9-11 show precisely the same general features as those presented earlier in the preceding section, where the lack of strong influence of this parameter was demonstrated conclusively. Figure 9 shows that, in absolute terms and quite consistent with the decreasing trend for mean velocity with increasing K_L, heat flux decreases steadily as the form loss coefficient is progressively increased. Consequently, mean temperatures for the guard vessel or collector wall increase monotonically with K_L, in line with the trends already established in Fig. 4. It is quite evident from Fig. 9 that values for wall heat flux are generally lower than 1 kW/ft^2 for all K_L when the average reactor vessel temperature is held constant at 1000°F. Also, when the results of Fig. 9 are expressed as the heat flux ratios (Table 2), it may be noted that the effect of K_L does not modify the conclusion drawn from the analysis with an assume heat flux, that is, the enhancement factor increase with increasing K_L over the range of values between K_L = 1 and K_L = 20, with almost no influence of e/D_h at a given K_L.

With a fixed reactor vessel temperature and relative to the results with the smooth duct option, the mean guard vessel temperatures are lowered by roughly a constant factor. For example, using the p/e = 10 results of Fig. 9, the percentage reductions can be stated as 47, 49, 47 and 44% for K_L = 1, 5,

10 and 20, successively. Also, using the p/e = 10 temperature data obtained for the conditions of Fig. 11, the average drop in mean guard vessel temperature was 43%, with a deviation of ±7% for 800°F ≤ $\bar{T}_{RV}$ ≤ 1400°F. By contrast, the collector wall temperatures were reduced by at least a factor of two. Also, as with the guard vessel, these factors varied slightly as the reactor vessel temperature is progressively increased.

With increasing reactor vessel temperature, the driving head in the heated or stack zone, the mass flowrate and system pressure losses increase markedly, due mainly to the generally expected effect of temperature on air density. Also, guard vessel heat flux must be expected to increase monotonically with reactor vessel temperature, and if heat transmission to the guard vessel is solely by radiation, then $\bar{T}_{RV} \propto Q_w^n$, where n = 0.25. Due to thermal resistances from the reactor vessel to the guard vessel and from the latter to the air, the value for n would probably be greater than 0.25. This dependence of Q_w on average reactor vessel temperature is strikingly illustrated in Fig. 11. Using the p/e = 10 data, a logarithmic best fit through the data gives $\bar{T}_{RV} \propto Q_w^n$, where n = 0.28, with a correlation coefficient that is better than 0.999. For the mean guard vessel temperature, the exponent on Q_w is 0.36.

It should be emphasized that these results with assumed values of reactor vessel temperature complement those already presented in the preceding section for specified wall flux, and that the two sets of results are satisfactorily consistent. For example, it can be established from Fig. 4(a) that $\bar{T}_{RV}$ is about 1070°F for K_L = 10 and p/e = 10. From Fig. 11(a) it may be noted that for this value of $\bar{T}_{RV}$ and p/e = 10, the heat flux is between 0.8 and 1.3 kW/ft^2, with an estimated value of 0.995 kW/ft^2; practically the same as the input value for the results of Fig. 4.

CONCLUSIONS

Analytical studies on the impact of roughness on the thermal performance of the LMR decay heat removal systems were made. The most significant conclusions can be summarized as follows:

1. For a specified guard vessel heat flux, reductions in mean wall temperatures of more than 200% can be obtained for the guard vessel and collector wall, provided that the ribs are located on both walls. For these conditions, the magnitudes of the reduction in mean reactor vessel temperature are equally significant, ranging from 30% to 100% for optimum pitch and flow attack angle.
2. For a specified reactor vessel temperature and with two rough walls, the heat flux that can be removed is nearly double that with the smooth duct option.
3. For $5 \leq p/e \leq 20$ and $0.026 \leq e/D_h \leq 0.103$, the fact that heat removal capability is almost independent of p/e or e/D_h is probably one of the most attractive features, inasmuch as this should afford greater flexibility in design as well as fabrication.
4. In the presence of repeated ribs, no significant benefits can be realized by reducing or increasing the guard vessel to collector wall gap size beyond the current value of 30.5 cm.
5. Preliminary results obtained with ribs only on the collector wall show moderate improvements in mean wall temperatures over the smooth duct option. With reliable predictive equations for friction and heat transfer in ducts with one rough wall, the conjecture is that this option might give heat removal capabilities that are at least 50-100% higher than with the smooth duct option. This is an area where further work is recommended.

ACKNOWLEDGEMENTS

This work was performed under the auspices of the U. S. Department of Energy, Office of Technology Support Programs, under contract W-31-109-Eng-38.

NOMENCLATURE

A_{fh}, A_{fs} = heated, stack zone cross-sectional area, m^2

B^+ = roughness function, Eq. (14)

C_p = specific heat, J/kg°C

D_h, D_{hs} = heated, stack zone hydraulic diameter, m

e = rib height, m

e^+ = roughness Reynolds number, Eq. (15)

f = Fanning friction factor

$\bar{f}$ = modified friction factor, Eq. (8)

G = mass flux, kg/m^2s

H = channel spacing or guard vessel to collector wall gap size, m

H^+ = heat transfer function, Eq. (16)

h = heat transfer coefficient, $W/m^2°C$

K_L = overall form loss coefficient in terms of heated zone inlet velocity head, Eq. (3)

k = air thermal conductivity, W/m°C

L_h, L_s = length of heated zone, stack length, m

Nu = Nusselt number, hD_h/k

$\bar{Nu}$ = modified Nusselt number, Eq. (9)

Pr = Prandtl number, $\mu C_p/k$

P_w = wetted perimeter, m

ΔP_{fh} = heated zone pressure loss, N/m^2

ΔP_h = thermal driving head, N/m^2

ΔP_L = system pressure losses, N/m^2

p = rib pitch, m

Q_w = heat flux, W/m^2

Re = Reynolds number, GD_h/μ

$\overline{Re}$ = modified Reynolds number, Eq. (10)

T = temperature, °C

$\overline{T}$ = average temperature, °C

W = channel width, m

α = flow attack angle, degrees

μ = air viscosity, kg/ms

ρ = air density, kg/m^3

$\overline{\rho}$ = average air density in heated zone, kg/m^3

ϕ = rib shape angle, degrees

Additional subscripts:

a = exit

CW = collector wall

GV = guard vessel

o = inlet

RV = reactor vessel

r; w,r = roughened duct

s; w,s = smooth duct

REFERENCES

Bird, R. B., Stewart, W. E., and Lightfoot, E. N., 1960, Transport Phenomena, John Wiley and Sons, NY, p. 217.

Gomelauri, V., 1964, "Influence of Two-Dimensional Artificial Roughness on Convective Heat Transfer," Int. J. Heat Mass Transfer, Vol. 7, pp. 653-663.

Han, J. C., and Park, J. S., 1986, "Local Heat Transfer in Channels with Two Opposite Ribbed Surfaces," in Heat Transfer 1986, Proc. 8th Int. Heat Transfer Conf., Vol. 6, pp. 2885-2890.

Han, J. C., Glicksman, L. R., and Rohsenow, W. M., 1979, "Correction to an Investigation of Heat Transfer and Friction for Rib-Roughened Surfaces," Int. J. Heat Mass Transfer, Vol. 22, pp. 1587-1588.

Han, J. C., Glicksman, L. R., and Rohsenow, W. M., 1978, "An Investigation of Heat Transfer and Friction for Rib-Roughened Surfaces," Int. J. Heat Mass Transfer, Vol. 21, pp. 1143-1156.

Jones, Jr., O. C., 1976, "An Improvement in the Calculation of Turbulent Friction in Rectangular Ducts," Trans. ASME J. Fluids Eng., Vol. 98, pp. 173-181.

Obot, N. T., 1987, "Determination of Incompressible Flow Friction in Smooth Circular and Noncircular Passages: A Generalized Approach Including Validation of the Nearly Century Old Hydraulic Diameter Concept," Submitted to Trans. ASME J. Fluids Eng.

Webb, R. L., Eckert, E. R. G., and Goldstein, R. J., 1971, "Heat Transfer and Friction in Tubes with Repeated-Rib Roughness," Int. J. Heat Mass Transfer, Vol. 14, pp. 601-617.

Vilemas, J. V., and Simonis, V. M., 1985, "Heat Transfer and Friction of Rough Ducts Carrying Gas Flow with Variable Physical Properties," Int. J. Heat Mass Transfer, Vol. 28, pp. 59-68.

Table 1. Parametric Ranges for the SHRS Analysis

Parameter	Range
Heated zone channel width	1.32 m
Stack zone channel width	1.32 m
Heated length	6.71 m
Stack height	18.0 m
NSTF heated zone cross-section	0.305 m x 1.32 m
Relative pitch, p/e	Smooth (p/e = 0) and $5 \leq p/e \leq 20$
Flow attack angle, α	Smooth ($\alpha = 0$) and $20 \leq \alpha \leq 90$ deg.
Relative rib height, e/D_h	Smooth ($e/D_h=0$) and $0.026 \leq e/D_h \leq 0.103$
Rib shape or profile angle, ϕ	90 degrees
Heated zone gap size	0.152-0.46 m
Form loss coefficient, K_L	$1 \leq K_L \leq 20$
Wall heat flux, Q_w (kW/m^2)	$1.1 \leq Q_w \leq 21.5$
Inlet air temperature	0°C, 21.1°C

Table 2. Effects of e/D_h and K_L on Heat Flux Ratios for $p/e = 10$ and $\bar{T}_{RV} = 1000°F$

	Heat Flux Ratio, $Q_{w,r}/Q_{w,s}$			
e/D_h (e, mm)	$K_L = 1$	$K_L = 5$	$K_L = 10$	$K_L = 20$
0.026 (12.7)	1.46	1.75	1.91	2.10
0.051 (25.4)	1.47	1.78	1.97	2.18
0.103 (50.8)	1.46	1.80	2.01	2.25

Figure Captions

Fig. 1. Cross-section of the annular flow passage.

Fig. 2. Variation of heated zone to total pressure loss with flow attack angle.

Fig. 3. Typical effect of rib height on mean guard vessel temperature.

Fig. 4. Typical effects of overall form loss coefficient on mean temperatures.

Fig. 5. Effect of guard vessel to collector wall gap size on mean temperatures for $K_L = 10$.

Fig. 6. Effect of guard vessel to collector wall gap size on mean temperatures with variable K_L.

Fig. 7. Variation of mean temperatures with heat flux and with Reynolds number.

Fig. 8. Mean guard vessel temperatures for smooth duct and with ribs on one wall and two walls.

Fig. 9. Effects of K_L on Q_w and mean guard vessel temperature with $\bar{T}_{RV} = 1000°F$.

Fig. 10. Effects of e/D_h on Q_w and mean temperatures with $\bar{T}_{RV} = 1000°F$.

Fig. 11. Variation of heat flux with p/e and $\bar{T}_{RV}$.

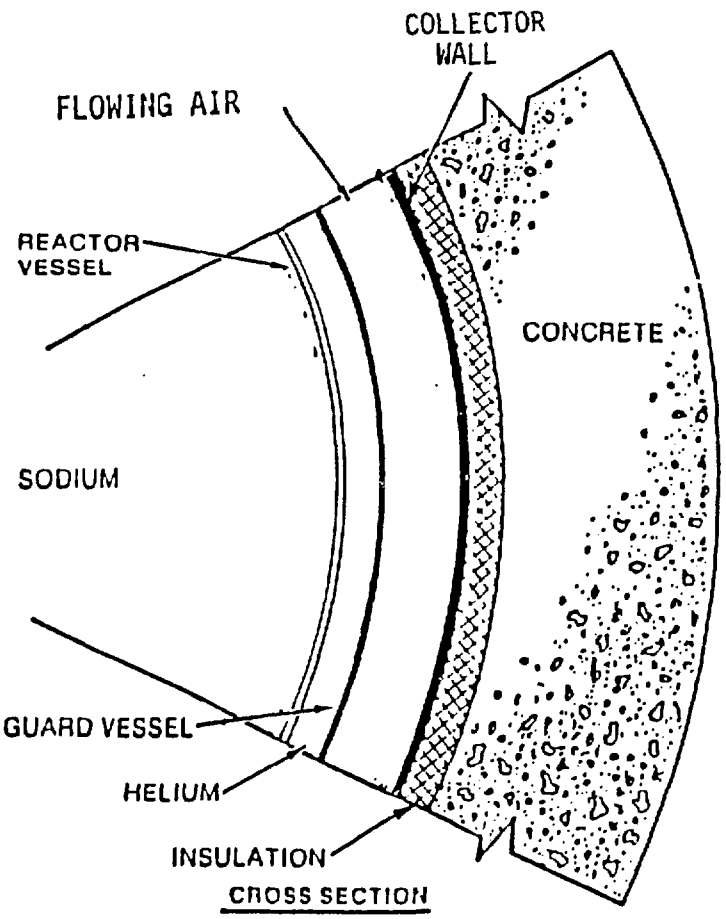
COLLECTOR
WALL
FLOWING AIR
REACTOR
VESSEL
CONCRETE
SODIUM
GUARD VESSEL
HELIUM
INSULATION
CROSS SECTION

Figure 1.

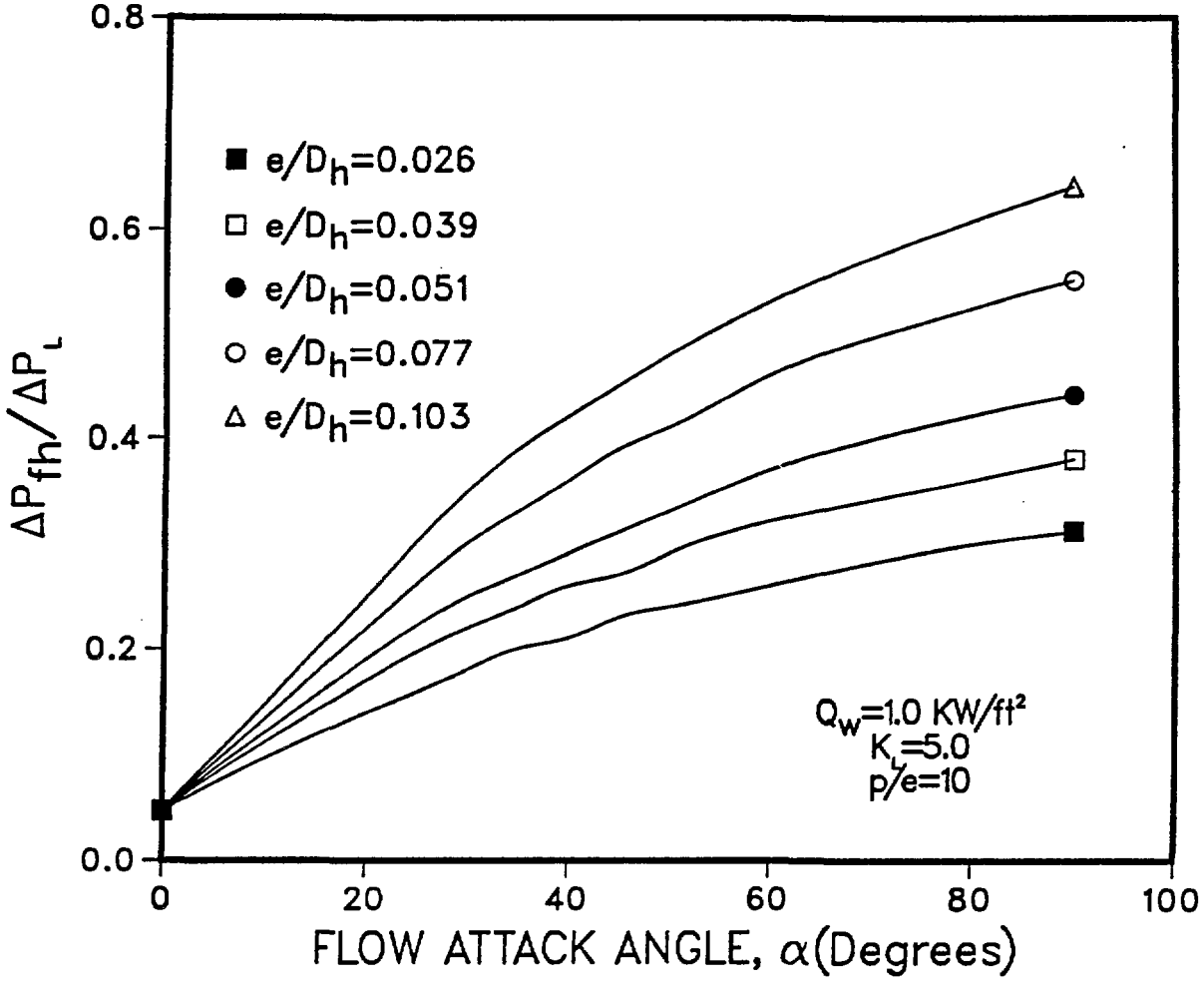
0.8
0.6
0.4
0.2
0.0
$\Delta P_{fh}/\Delta P_L$
■ e/D_h=0.026
□ e/D_h=0.039
● e/D_h=0.051
○ e/D_h=0.077
△ e/D_h=0.103
Q_w=1.0 KW/ft²
K_L=5.0
p/e=10
0
20
40
60
80
100
FLOW ATTACK ANGLE, α(Degrees)

Figure 2.

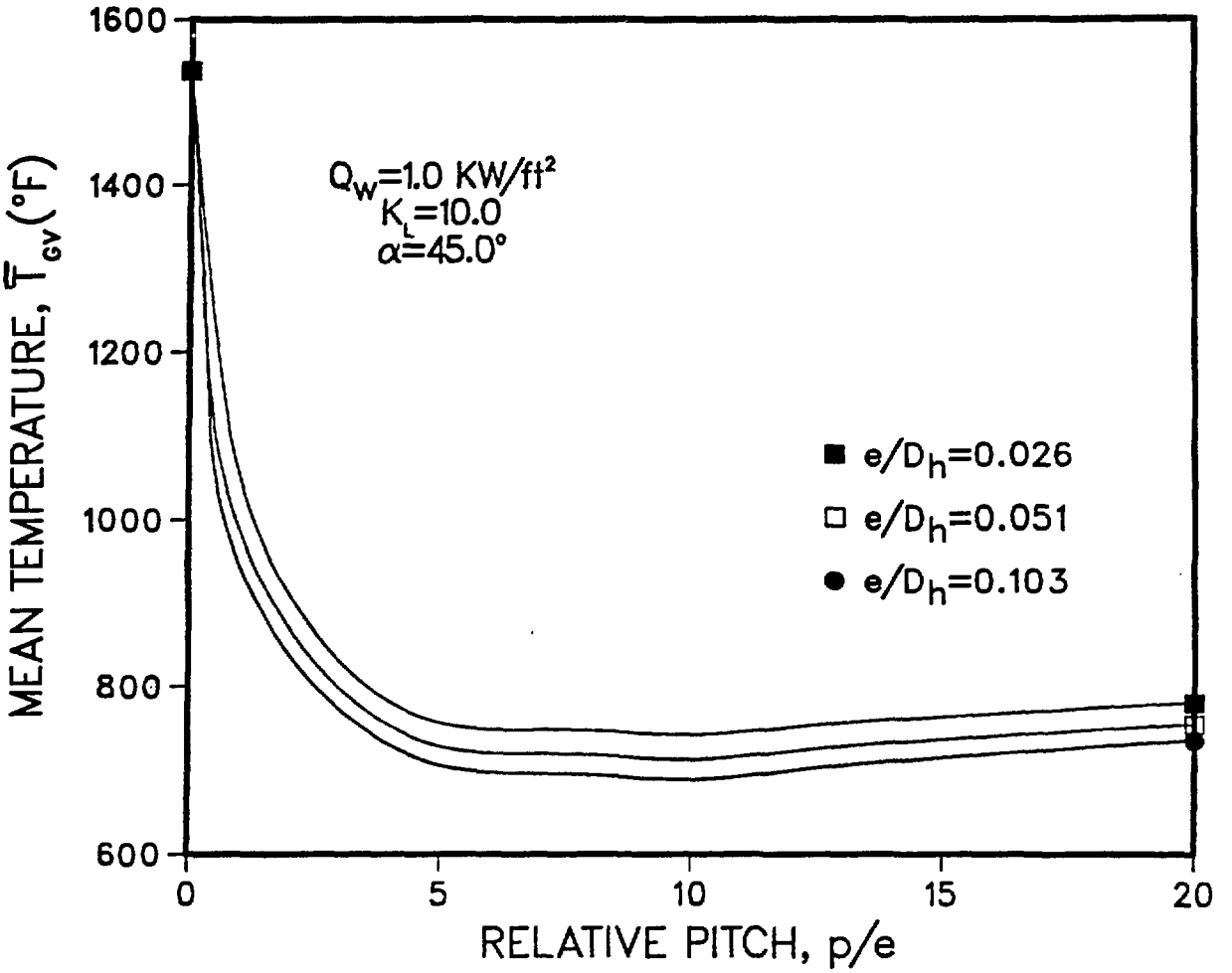
1600
1400
1200
1000
800
600
0
5
10
15
20
MEAN TEMPERATURE, $\bar{T}_{gv}$(°F)
RELATIVE PITCH, p/e
Q_w=1.0 KW/ft²
K_L=10.0
α=45.0°
■ e/D_h=0.026
□ e/D_h=0.051
● e/D_h=0.103

Figure 3.

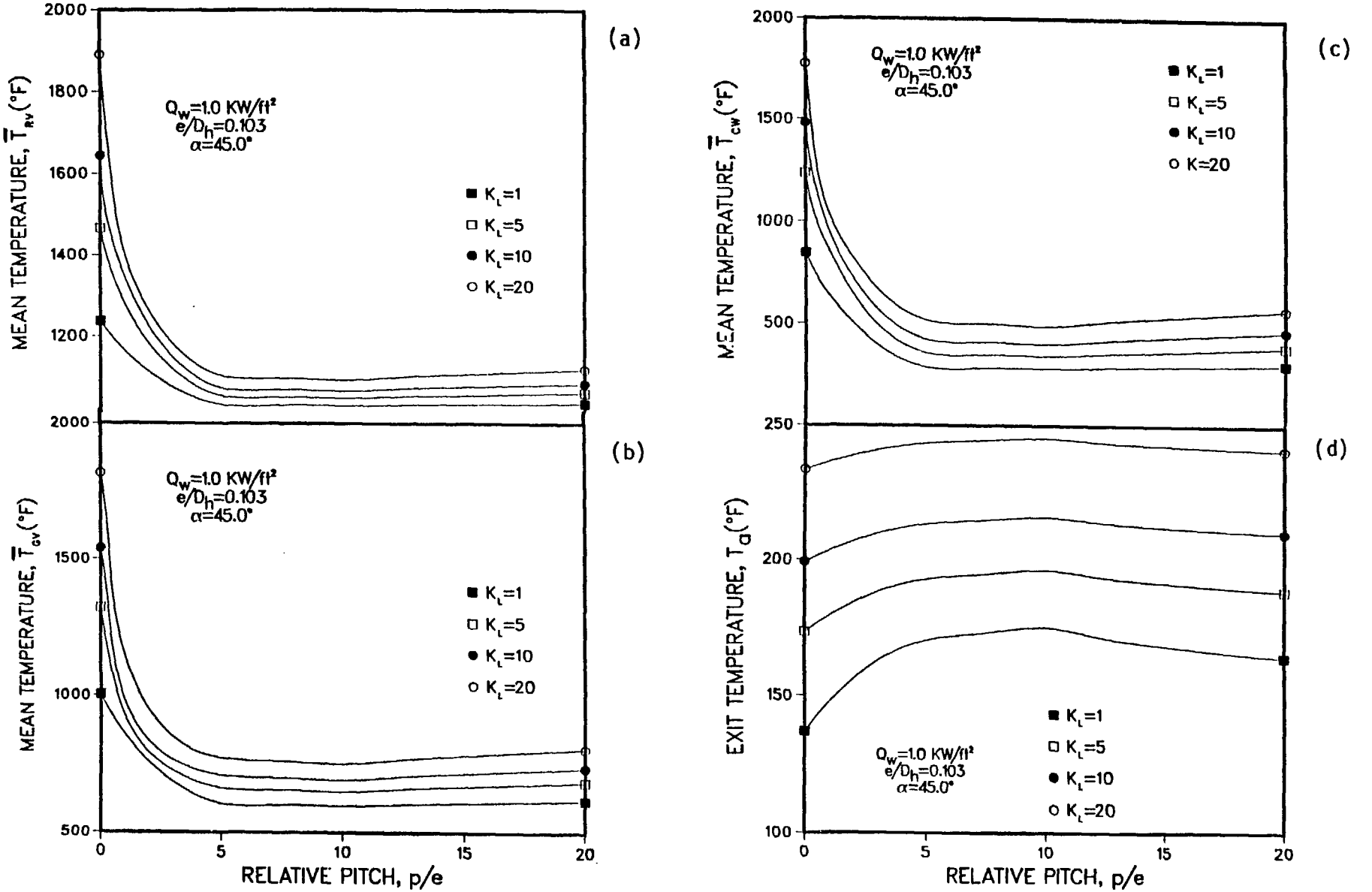
(a)
(b)
(c)
(d)
Q_w=1.0 KW/ft²
e/D_h=0.103
α=45.0°
K_L=1
K_L=5
K_L=10
K_L=20
K=20
MEAN TEMPERATURE, $\bar{T}_{av}$(°F)
MEAN TEMPERATURE, $\bar{T}_{cv}$(°F)
MEAN TEMPERATURE, $\bar{T}_{cw}$(°F)
EXIT TEMPERATURE, T_a(°F)
RELATIVE PITCH, p/e
2000
1800
1600
1400
1200
1500
1000
500
1500
1000
250
200
150
100
0
5
10
15
20

Figure 4.

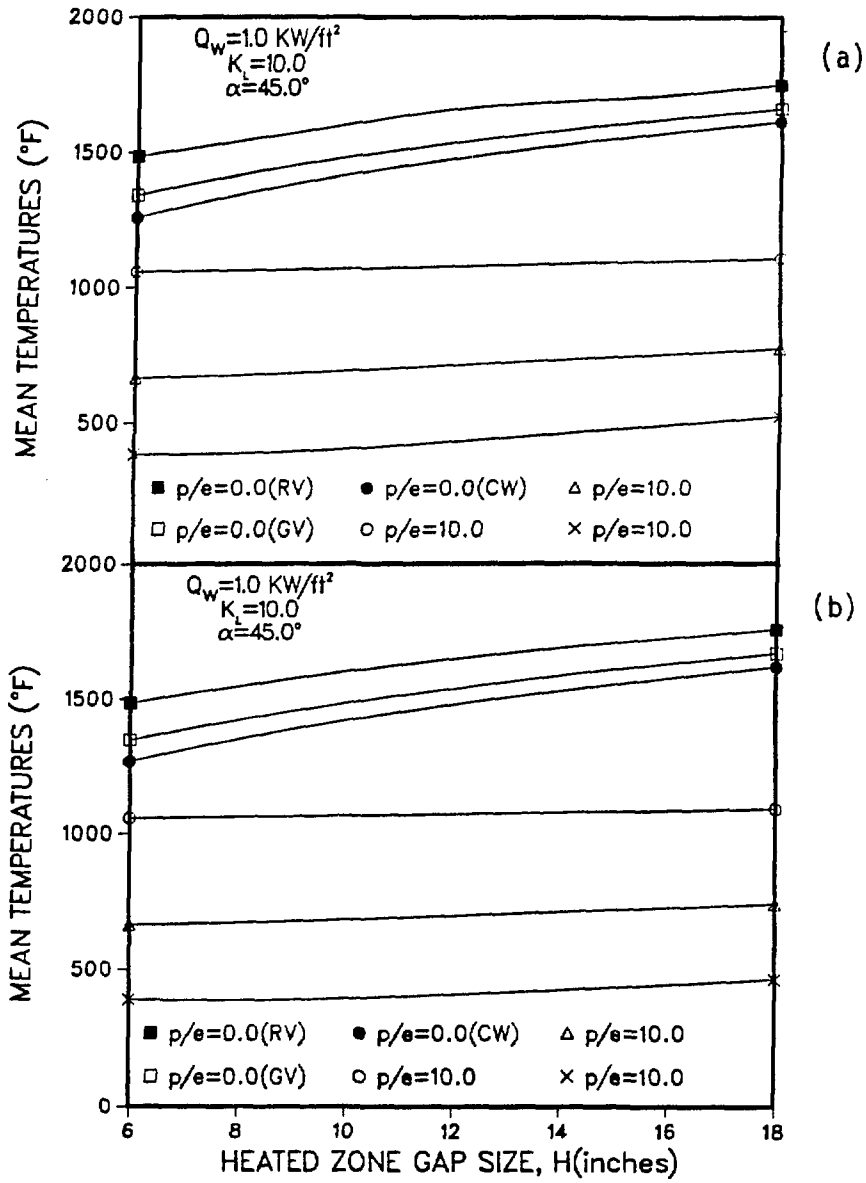
(a)
Q_w=1.0 KW/ft²
K_L=10.0
α=45.0°
MEAN TEMPERATURES (°F)
2000
1500
1000
500
■ p/e=0.0(RV)
● p/e=0.0(CW)
△ p/e=10.0
□ p/e=0.0(GV)
○ p/e=10.0
× p/e=10.0
(b)
Q_w=1.0 KW/ft²
K_L=10.0
α=45.0°
MEAN TEMPERATURES (°F)
2000
1500
1000
500
0
■ p/e=0.0(RV)
● p/e=0.0(CW)
△ p/e=10.0
□ p/e=0.0(GV)
○ p/e=10.0
× p/e=10.0
6
8
10
12
14
16
18
HEATED ZONE GAP SIZE, H(inches)

Figure 5.

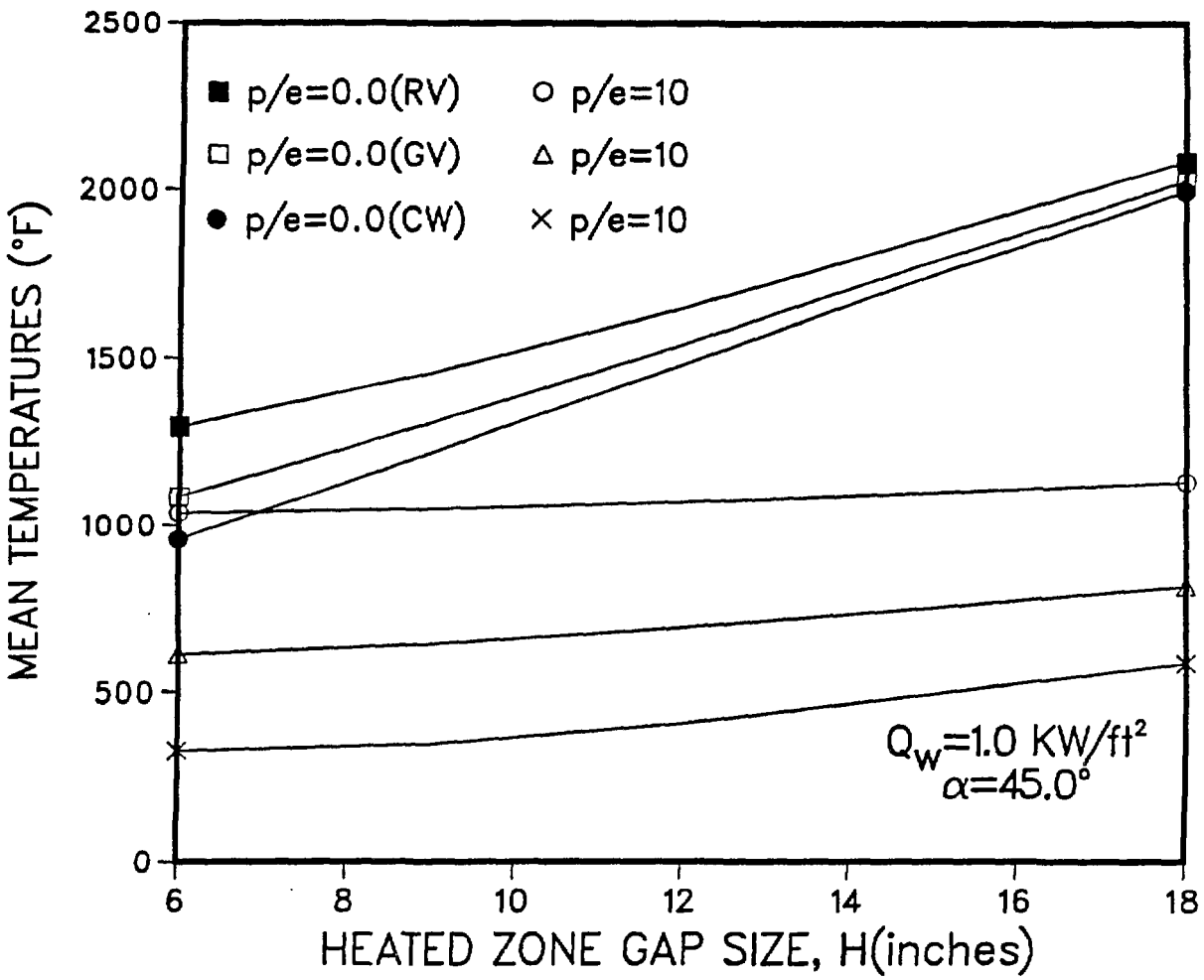
2500
2000
1500
1000
500
0
MEAN TEMPERATURES (°F)
■ p/e=0.0(RV)
□ p/e=0.0(GV)
● p/e=0.0(CW)
○ p/e=10
△ p/e=10
× p/e=10
Q_w=1.0 KW/ft²
α=45.0°
6
8
10
12
14
16
18
HEATED ZONE GAP SIZE, H(inches)

Figure 6.

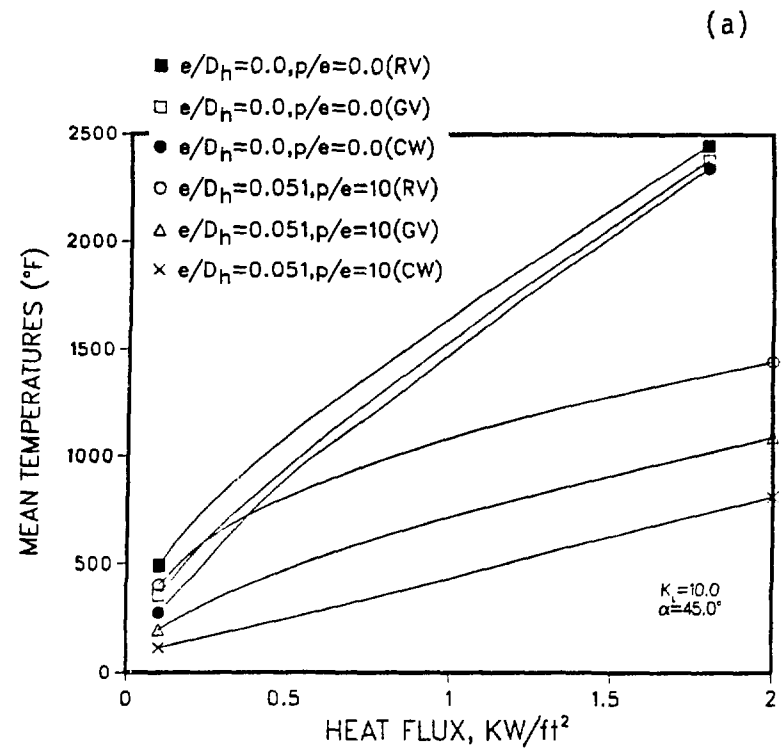
(a)
■ e/Dh=0.0,p/e=0.0(RV)
□ e/Dh=0.0,p/e=0.0(GV)
● e/Dh=0.0,p/e=0.0(CW)
○ e/Dh=0.051,p/e=10(RV)
△ e/Dh=0.051,p/e=10(GV)
× e/Dh=0.051,p/e=10(CW)
MEAN TEMPERATURES (°F)
2500
2000
1500
1000
500
0
0
0.5
1
1.5
2
HEAT FLUX, KW/ft²
KL=10.0
α=45.0°

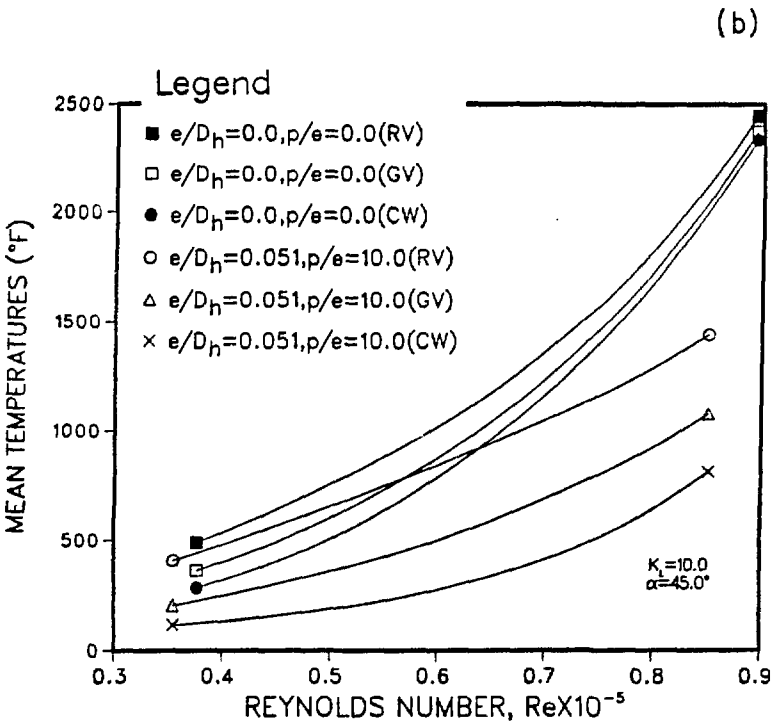
(b)
Legend
■ e/Dh=0.0,p/e=0.0(RV)
□ e/Dh=0.0,p/e=0.0(GV)
● e/Dh=0.0,p/e=0.0(CW)
○ e/Dh=0.051,p/e=10.0(RV)
△ e/Dh=0.051,p/e=10.0(GV)
× e/Dh=0.051,p/e=10.0(CW)
MEAN TEMPERATURES (°F)
2500
2000
1500
1000
500
0
0.3
0.4
0.5
0.6
0.7
0.8
0.9
REYNOLDS NUMBER, ReX10⁻⁵
KL=10.0
α=45.0°

Figure 7.

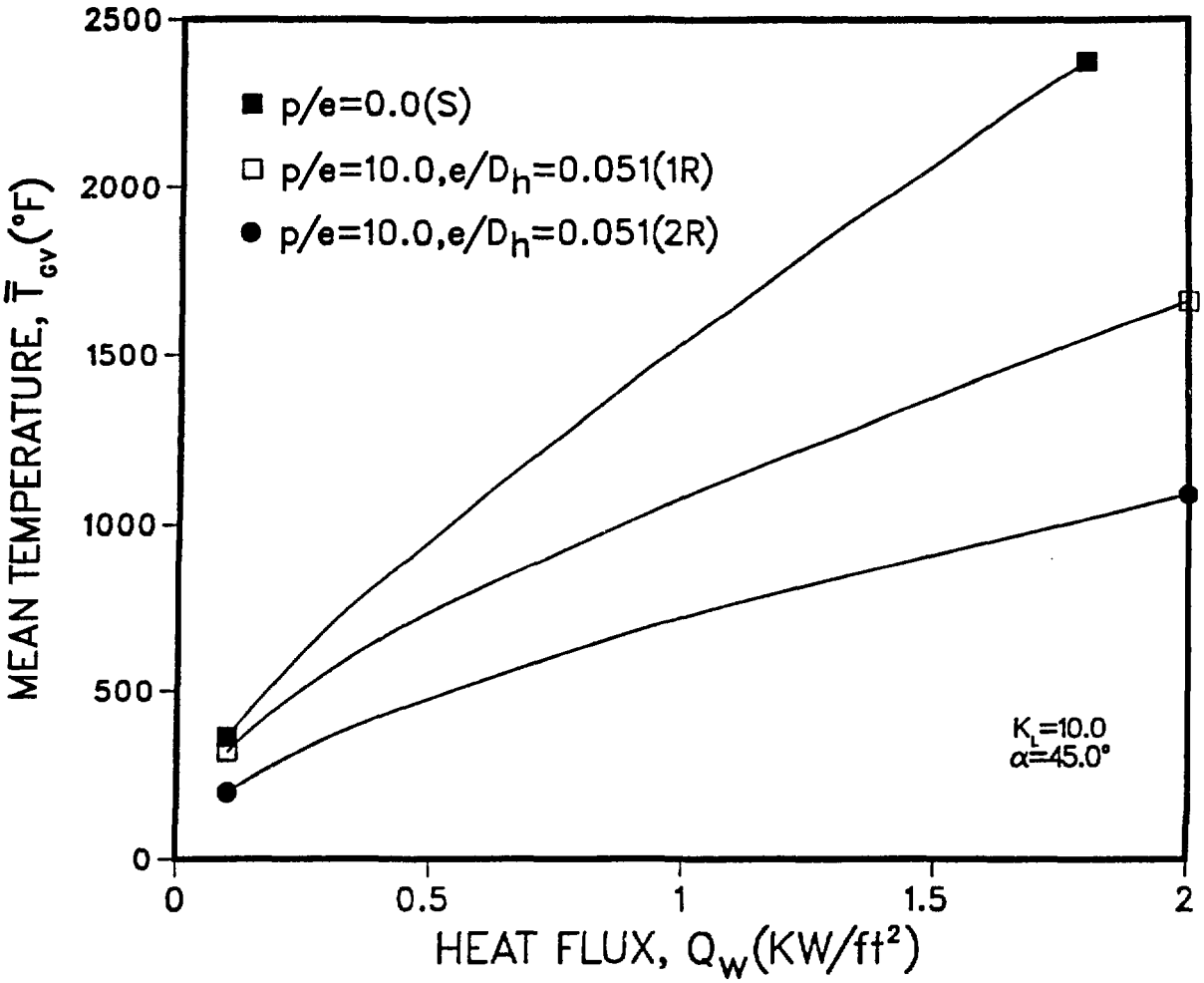
2500
2000
1500
1000
500
0
MEAN TEMPERATURE, $\bar{T}_{GV}$(°F)
■ p/e=0.0(S)
□ p/e=10.0,e/D_h=0.051(1R)
● p/e=10.0,e/D_h=0.051(2R)
K_L=10.0
α=45.0°
0
0.5
1
1.5
2
HEAT FLUX, Q_w(KW/ft²)

Figure 8.

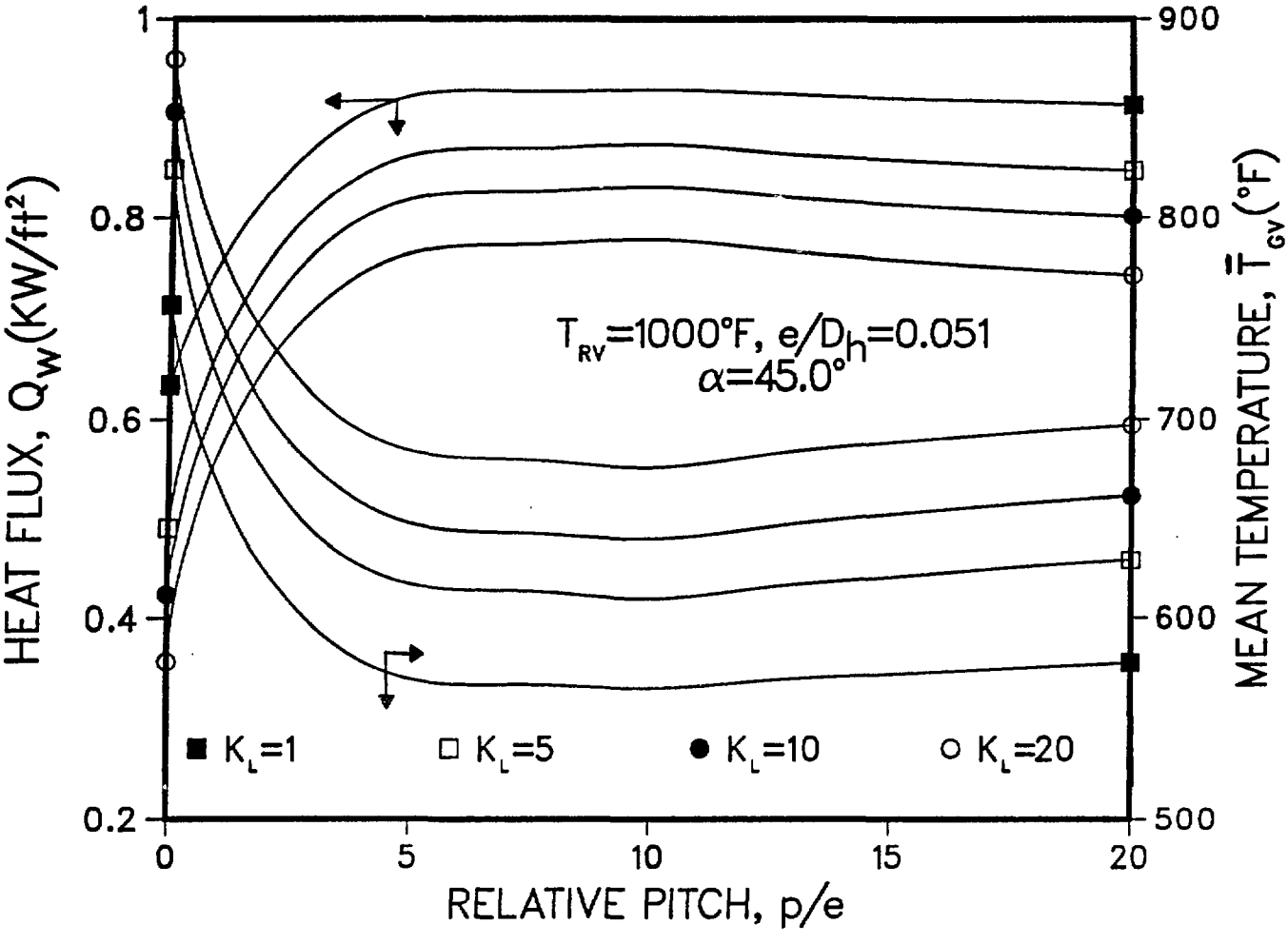
HEAT FLUX, Q_w(KW/ft²)
MEAN TEMPERATURE, $\bar{T}_{GV}$(°F)
RELATIVE PITCH, p/e
T_{RV}=1000°F, e/D_h=0.051
α=45.0°
K_L=1
K_L=5
K_L=10
K_L=20
1
0.8
0.6
0.4
0.2
900
800
700
600
500
0
5
10
15
20

Figure 9.

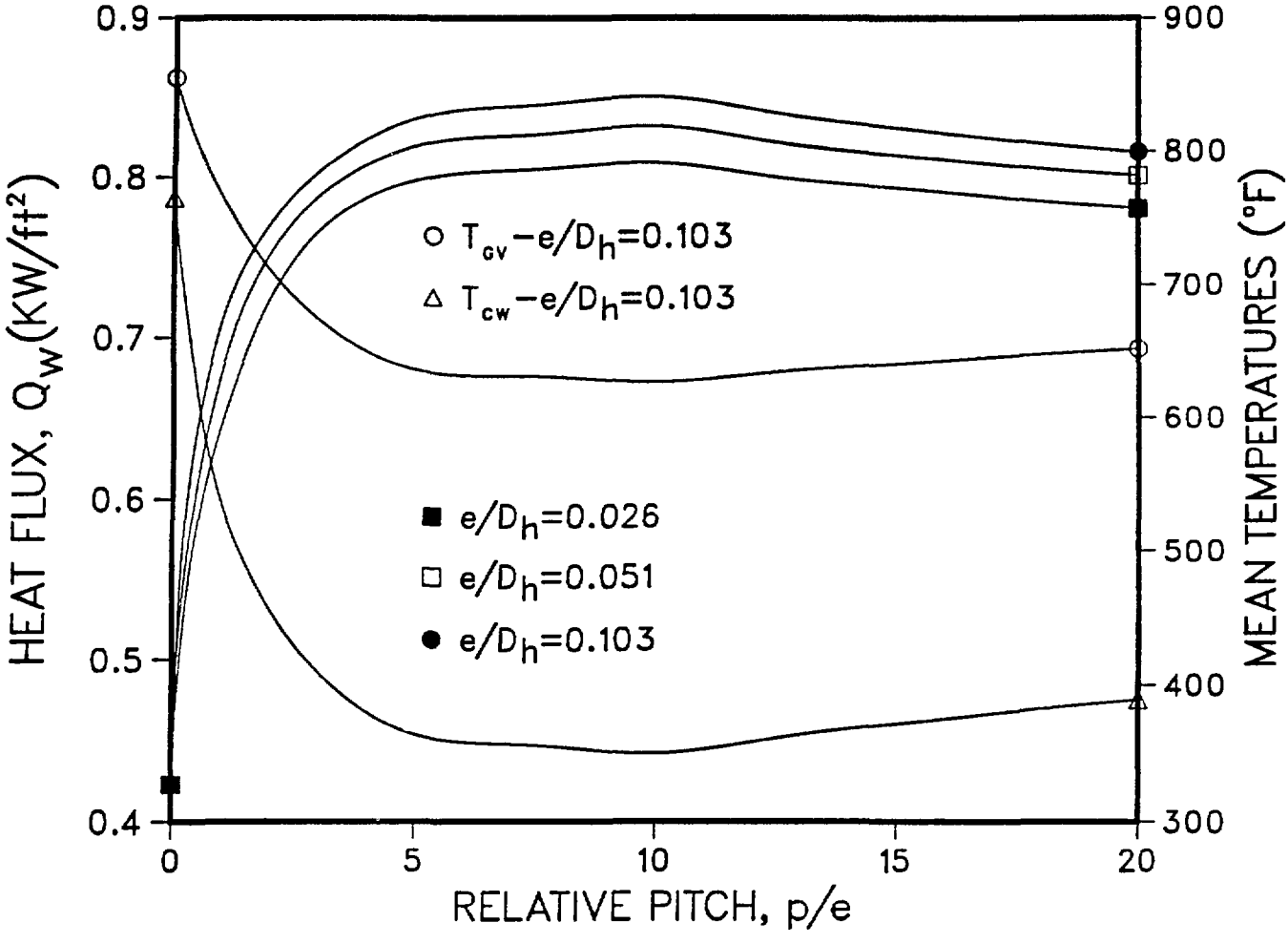
0.9
0.8
0.7
0.6
0.5
0.4
900
800
700
600
500
400
300
0
5
10
15
20
HEAT FLUX, Q_w(KW/ft²)
MEAN TEMPERATURES (°F)
RELATIVE PITCH, p/e
○ T_{cv} – e/D_h=0.103
△ T_{cw} – e/D_h=0.103
■ e/D_h=0.026
□ e/D_h=0.051
● e/D_h=0.103

Figure 10.

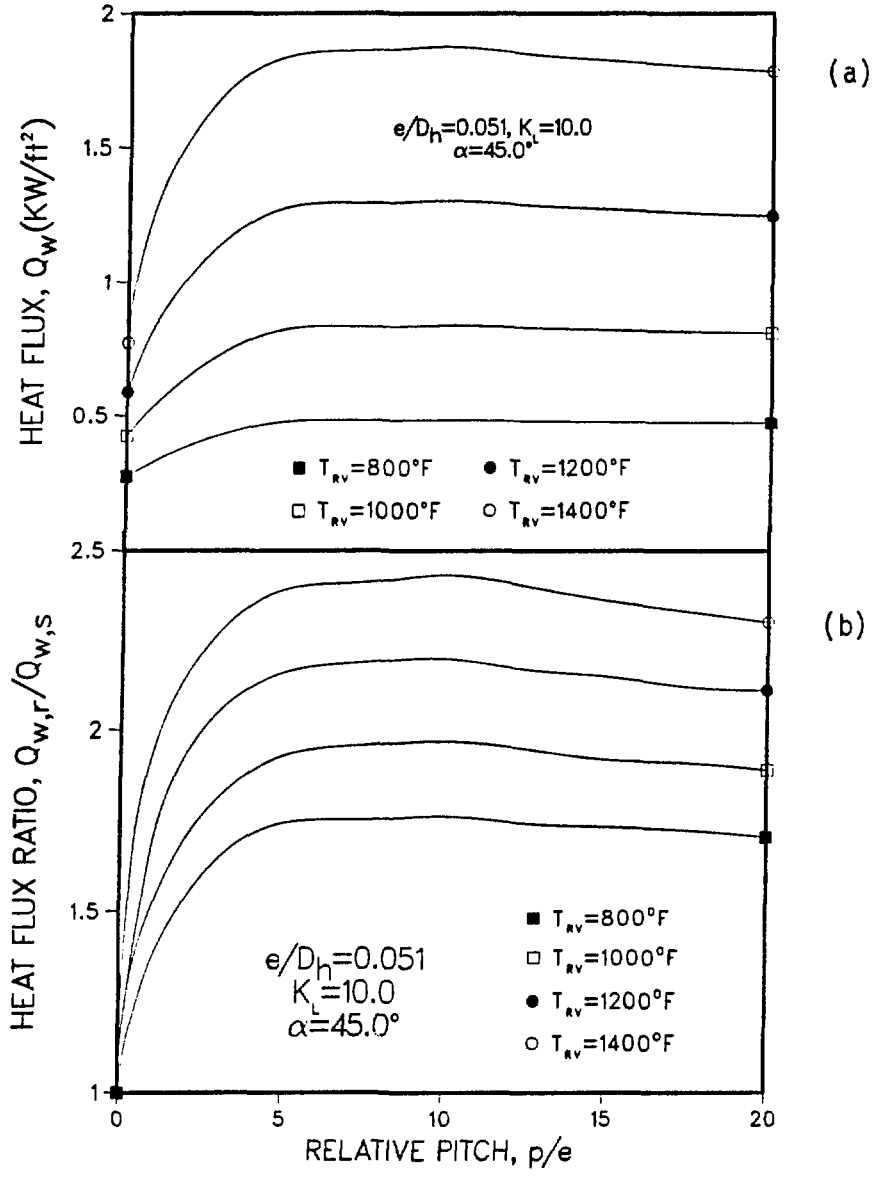
(a)
HEAT FLUX, Q_w(KW/ft²)
e/D_h=0.051, K_L=10.0
α=45.0°
■ T_{RV}=800°F
● T_{RV}=1200°F
□ T_{RV}=1000°F
○ T_{RV}=1400°F
(b)
HEAT FLUX RATIO, $Q_{w,r}/Q_{w,s}$
e/D_h=0.051
K_L=10.0
α=45.0°
■ T_{RV}=800°F
□ T_{RV}=1000°F
● T_{RV}=1200°F
○ T_{RV}=1400°F
RELATIVE PITCH, p/e

Figure 11.